

# Role of quark-interchange processes in evolution of mesonic matter

Yu-Qi Li      Xiao-Ming Xu      Hui-Jun Ge

*Department of Physics, Shanghai University, Baoshan, Shanghai 200444, China*

## Abstract

We divide the cross section for a meson-meson reaction into three parts. The first part is for the quark-interchange process, the second for quark-antiquark annihilation processes and the third for resonant processes. Master rate equations are established to yield time dependence of fugacities of pions, rhos, kaons and vector kaons. The equations include cross sections for inelastic scattering of pions, rhos, kaons and vector kaons. Cross sections for quark-interchange-induced reactions, that were obtained in a potential model, are parametrized for convenient use. The number densities of  $\pi$  and  $\rho$  ( $K$  and  $K^*$ ) are altered by quark-interchange processes in equal magnitudes but opposite signs. The master rate equations combined with the hydrodynamic equations for longitudinal and transverse expansion are solved with many sets of initial meson fugacities. Quark-interchange processes are shown to be important in the contribution of the inelastic meson-meson scattering to evolution of mesonic matter.

PACS: 25.75.-q; 13.75.Lb; 25.75.Dw

Keywords: quark-interchange processes, master rate equations, mesonic matter

# 1 Introduction

Deconfined matter with high temperature and high density is the focus of studies in ultrarelativistic heavy-ion collisions and its confirmation is well known to be related to final-state observables. But hadronic observables are affected by hadronic matter that succeeds deconfined matter and measurements on dileptons and photons suffer from a background that comes from hadronic matter. In order to clearly identify deconfined matter from hadronic observables and electromagnetic probes, one has to subtract any influence of hadronic matter. This forces us to pursue a precise description of hadronic matter. In addition, a complete knowledge of ultrarelativistic heavy-ion collisions also requires understanding of the evolution of hadronic matter.

Transport models [1–14] can provide with vivid and valid descriptions for the evolution of hadronic matter. The models deal with known and unknown cross sections for hadron-hadron reactions in the following ways. If experimental data are available, parametrizations fitted to the data are first used. If no measured data exist, cross sections can stem from theoretical calculations, are simply assumed to be constants, are adapted to the Breit-Wigner formula with hypothetical widths, or are obtained from the parametrizations via the detailed balance or via approximate isospin relations. Features of a sort of reactions can be definitely shown by the parametrizations that depend on threshold energies and the center-of-mass energy of the two colliding hadrons. The assumptions of constant cross sections and the approximate isospin relations bring uncertainties to study of the evolution of hadronic matter and predictions on final-state observables.

Time evolution of meson density, for example,  $\phi$  meson density [15], can be studied with a rate equation that includes cross sections for scattering of the meson by other hadrons. The number of necessary cross sections is huge if rate equations for many hadrons are established. To avoid complexity caused by a great number of mesonic degrees of freedom in hadronic matter, effective numbers of pions and kaons were introduced to approximately get evolution of pionic matter and kaonic matter [16–18]. The effective number of pions (kaons) is defined as the number of pions (kaons) plus the sum of other hadrons weighted by their effective pionic (kaonic) content. For instance, a  $\rho$  meson counts as two pions and an  $\Omega$  baryon counts as three kaons. With this consideration rate equations for the effective numbers of pions and kaons were established [16–18].

At mid-rapidity the PHENIX Collaboration [19] obtained ratios of  $p_T$ -integrated meson yields in central Au+Au collisions at  $\sqrt{s_{NN}}=200$  GeV as follows:  $\pi^-/\pi^+ = 0.984$ ,  $K^-/K^+ = 0.933$ ,  $K^+/\pi^+ = 0.171$  and  $K^-/\pi^- = 0.162$ , which agree with the results of the other collaborations [20–22]. The STAR Collaboration found  $\rho^0/\pi^- = 0.169$  in

peripheral Au+Au collisions at  $\sqrt{s_{NN}} = 200$  GeV [23]. Obviously, pions, rhos and kaons are dominant meson species in hadronic matter. In the present work we consider only pions, rhos, kaons and vector kaons that constitute mesonic matter. Inelastic meson-meson scattering originates from resonances, quark-antiquark annihilation processes and quark-interchange processes. At the lowest order a resonance is made up of the remaining quark and antiquark of which one absorbs a gluon from the annihilation of a quark in an initial meson and an antiquark in another initial meson. Of course resonances may be glueballs, multiquark states or hybrid states [24, 25]. At the lowest order the quark-antiquark annihilation means that a quark and an antiquark each in a final meson come from the annihilation of a quark and an antiquark each in an initial meson. A quark-interchange process allows such a type of meson-meson scattering where one gluon exchange and the interchange of two quarks each from an initial meson happen. One is acquainted with the inelastic meson-meson scattering due to the resonance and the quark-antiquark annihilation, but not the scattering induced by the quark interchange. One also doesn't know how important the scattering induced by the quark interchange is in the evolution of mesonic matter. Indeed, nobody had calculated cross sections for the seven quark-interchange-induced reactions  $\pi\pi \leftrightarrow \rho\rho$  for  $I = 2$ ,  $KK \leftrightarrow K^*K^*$  for  $I = 1$ ,  $KK^* \leftrightarrow K^*K^*$  for  $I = 1$ ,  $\pi K \leftrightarrow \rho K^*$  for  $I = \frac{3}{2}$ ,  $\pi K^* \leftrightarrow \rho K^*$  for  $I = \frac{3}{2}$ ,  $\rho K \leftrightarrow \rho K^*$  for  $I = \frac{3}{2}$  and  $\pi K^* \leftrightarrow \rho K$  for  $I = \frac{3}{2}$ , until we obtained cross sections for these reactions in Ref. [26] in the quark-interchange mechanism [27, 28]. Therefore, we curiously study the role of quark-interchange processes that lead to the seven reactions and other isospin channels in the evolution of mesonic matter in the present work. The study resorts to master rate equations for mesons where reactions of pions, rhos, kaons and vector kaons are taken into account. It will be shown that quark-interchange processes are important in the contribution of the inelastic meson-meson scattering to the evolution of mesonic matter. Therefore, if we include the resonances and the quark-antiquark annihilation processes, the quark-interchange processes should be included on an equal footing.

In the next section the master rate equations for pions, rhos, kaons and vector kaons are established while the inelastic meson-meson scattering due to the resonance, the quark-antiquark annihilation and the quark interchange is considered. In Section 3 parametrizations of cross sections for the quark-interchange-induced reactions are presented. Cross sections for the quark-antiquark annihilation processes and the resonant processes are individually introduced. Numerical results of the master rate equations associated with longitudinal expansion and discussions are given in Section 4. The master rate equations are extended to include  $2 \leftrightarrow 1$  mesonic processes in Section 5 and in the case of both the

longitudinal and transverse expansion the importance of the quark-interchange processes is examined in Section 6. Summary is in the last section.

## 2 Master rate equations

We establish the notation  $K = \begin{pmatrix} K^+ \\ K^0 \end{pmatrix}$  and  $\bar{K} = \begin{pmatrix} \bar{K}^0 \\ K^- \end{pmatrix}$  for the pseudoscalar isospin doublets as well as  $K^* = \begin{pmatrix} K^{*+} \\ K^{*0} \end{pmatrix}$  and  $\bar{K}^* = \begin{pmatrix} \bar{K}^{*0} \\ K^{*-} \end{pmatrix}$  for the vector isospin doublets. We only consider  $\pi$ ,  $\rho$ ,  $K$ ,  $\bar{K}$ ,  $K^*$  and  $\bar{K}^*$  of mesonic matter. In order to clearly exhibit the role of the quark-interchange processes, we neglect both  $2 \rightarrow 1$  mesonic reactions and decays of  $\rho$ ,  $K^*$  and  $\bar{K}^*$  in this section and the next two sections. The negligence does not affect us to draw correct conclusions. The inclusion of the  $2 \leftrightarrow 1$  mesonic processes is deferred to Section 5. The reactions that can change the numbers of  $\pi$ ,  $\rho$ ,  $K$ ,  $\bar{K}$ ,  $K^*$  and  $\bar{K}^*$  in a lifetime of mesonic matter are the following inelastic 2-to-2 scattering:

1.  $\pi\pi \leftrightarrow \rho\rho$ ,
2.  $KK \leftrightarrow K^*K^*$  and  $\bar{K}\bar{K} \leftrightarrow \bar{K}^*\bar{K}^*$ ,
3.  $KK^* \leftrightarrow K^*K^*$  and  $\bar{K}\bar{K}^* \leftrightarrow \bar{K}^*\bar{K}^*$ ,
4.  $K\bar{K} \leftrightarrow K^*\bar{K}^*$ ,
5.  $K\bar{K}^* \leftrightarrow K^*\bar{K}^*$  and  $K^*\bar{K} \leftrightarrow K^*\bar{K}^*$ ,
6.  $\pi K^* \leftrightarrow \rho K$  and  $\pi \bar{K}^* \leftrightarrow \rho \bar{K}$ ,
7.  $\pi K \leftrightarrow \rho K^*$  and  $\pi \bar{K} \leftrightarrow \rho \bar{K}^*$ ,
8.  $\pi K^* \leftrightarrow \rho K^*$  and  $\pi \bar{K}^* \leftrightarrow \rho \bar{K}^*$ ,
9.  $\rho K \leftrightarrow \rho K^*$  and  $\rho \bar{K} \leftrightarrow \rho \bar{K}^*$ ,
10.  $\pi\pi \leftrightarrow K\bar{K}$ ,
11.  $\pi\rho \leftrightarrow K\bar{K}^*$  and  $\pi\rho \leftrightarrow K^*\bar{K}$ ,
12.  $K\bar{K} \leftrightarrow \rho\rho$ .

The cross sections for these reactions are not independent of each other, e.g.,  $\sigma_{\bar{K}\bar{K} \rightarrow \bar{K}^* \bar{K}^*} = \sigma_{KK \rightarrow K^* K^*}$ ,  $\sigma_{\bar{K}\bar{K}^* \rightarrow \bar{K}^* \bar{K}} = \sigma_{KK^* \rightarrow K^* K}$ ,  $\sigma_{K^* \bar{K} \rightarrow K^* \bar{K}} = \sigma_{K\bar{K}^* \rightarrow K^* \bar{K}^*}$ ,  $\sigma_{\pi \bar{K}^* \rightarrow \rho \bar{K}} = \sigma_{\pi K^* \rightarrow \rho K}$ ,  $\sigma_{\pi \bar{K} \rightarrow \rho \bar{K}^*} = \sigma_{\pi K \rightarrow \rho K^*}$ ,  $\sigma_{\pi \bar{K}^* \rightarrow \rho \bar{K}^*} = \sigma_{\pi K^* \rightarrow \rho K^*}$ ,  $\sigma_{\rho \bar{K} \rightarrow \rho \bar{K}^*} = \sigma_{\rho K \rightarrow \rho K^*}$ , and  $\sigma_{\pi \rho \rightarrow K^* \bar{K}} = \sigma_{\pi \rho \rightarrow K \bar{K}^*}$ .

Meson number densities change with time according to the following rate equations,

$$\partial_\mu (n_i u^\mu) = \Psi_i, \quad (1)$$

where  $u^\mu = (u^0, \vec{u}) = \gamma(1, \vec{v})$  is the four-velocity of the local reference frame comoving at velocity  $\vec{v}$  and with the Lorentz factor  $\gamma$ .  $n_\pi$ ,  $n_\rho$ ,  $n_K$ ,  $n_{\bar{K}}$ ,  $n_{K^*}$  and  $n_{\bar{K}^*}$  are the number densities of  $\pi$ ,  $\rho$ ,  $K$ ,  $\bar{K}$ ,  $K^*$  and  $\bar{K}^*$  if  $i$  denotes  $\pi$ ,  $\rho$ ,  $K$ ,  $\bar{K}$ ,  $K^*$  and  $\bar{K}^*$ , respectively. Zero values of the source terms  $\Psi_i$  mean that the total number of each particle species is conserved. The source terms are given by

$$\begin{aligned} \Psi_\pi = & 2 \times \frac{1}{2} \langle \sigma_{\rho\rho \rightarrow \pi\pi} v_{\rho\rho} \rangle n_\rho^2 - 2 \times \frac{1}{2} \langle \sigma_{\pi\pi \rightarrow \rho\rho} v_{\pi\pi} \rangle n_\pi^2 \\ & + \langle \sigma_{\rho K \rightarrow \pi K^*} v_{\rho K} \rangle n_\rho n_K - \langle \sigma_{\pi K^* \rightarrow \rho K} v_{\pi K^*} \rangle n_\pi n_{K^*} \\ & + \langle \sigma_{\rho \bar{K} \rightarrow \pi \bar{K}^*} v_{\rho \bar{K}} \rangle n_\rho n_{\bar{K}} - \langle \sigma_{\pi \bar{K}^* \rightarrow \rho \bar{K}} v_{\pi \bar{K}^*} \rangle n_\pi n_{\bar{K}^*} \\ & + \langle \sigma_{\rho K^* \rightarrow \pi K} v_{\rho K^*} \rangle n_\rho n_{K^*} - \langle \sigma_{\pi K \rightarrow \rho K^*} v_{\pi K} \rangle n_\pi n_K \\ & + \langle \sigma_{\rho \bar{K}^* \rightarrow \pi \bar{K}} v_{\rho \bar{K}^*} \rangle n_\rho n_{\bar{K}^*} - \langle \sigma_{\pi \bar{K} \rightarrow \rho \bar{K}^*} v_{\pi \bar{K}} \rangle n_\pi n_{\bar{K}} \\ & + \langle \sigma_{\rho K^* \rightarrow \pi K^*} v_{\rho K^*} \rangle n_\rho n_{K^*} - \langle \sigma_{\pi K^* \rightarrow \rho K^*} v_{\pi K^*} \rangle n_\pi n_{K^*} \\ & + \langle \sigma_{\rho \bar{K}^* \rightarrow \pi \bar{K}^*} v_{\rho \bar{K}^*} \rangle n_\rho n_{\bar{K}^*} - \langle \sigma_{\pi \bar{K}^* \rightarrow \rho \bar{K}^*} v_{\pi \bar{K}^*} \rangle n_\pi n_{\bar{K}^*} \\ & + 2 \langle \sigma_{K\bar{K} \rightarrow \pi\pi} v_{K\bar{K}} \rangle n_K n_{\bar{K}} - 2 \times \frac{1}{2} \langle \sigma_{\pi\pi \rightarrow K\bar{K}} v_{\pi\pi} \rangle n_\pi^2 \\ & + \langle \sigma_{K\bar{K}^* \rightarrow \pi\rho} v_{K\bar{K}^*} \rangle n_K n_{\bar{K}^*} - \langle \sigma_{\pi\rho \rightarrow K\bar{K}^*} v_{\pi\rho} \rangle n_\pi n_\rho \\ & + \langle \sigma_{K^* \bar{K} \rightarrow \pi\rho} v_{K^* \bar{K}} \rangle n_{K^*} n_{\bar{K}} - \langle \sigma_{\pi\rho \rightarrow K^* \bar{K}} v_{\pi\rho} \rangle n_\pi n_\rho, \end{aligned} \quad (2)$$

$$\begin{aligned}
\Psi_\rho = & 2 \times \frac{1}{2} \langle \sigma_{\pi\pi \rightarrow \rho\rho} v_{\pi\pi} \rangle n_\pi^2 - 2 \times \frac{1}{2} \langle \sigma_{\rho\rho \rightarrow \pi\pi} v_{\rho\rho} \rangle n_\rho^2 \\
& + \langle \sigma_{\pi K^* \rightarrow \rho K} v_{\pi K^*} \rangle n_\pi n_{K^*} - \langle \sigma_{\rho K \rightarrow \pi K^*} v_{\rho K} \rangle n_\rho n_K \\
& + \langle \sigma_{\pi \bar{K}^* \rightarrow \rho \bar{K}} v_{\pi \bar{K}^*} \rangle n_\pi n_{\bar{K}^*} - \langle \sigma_{\rho \bar{K} \rightarrow \pi \bar{K}^*} v_{\rho \bar{K}} \rangle n_\rho n_{\bar{K}} \\
& + \langle \sigma_{\pi K \rightarrow \rho K^*} v_{\pi K} \rangle n_\pi n_K - \langle \sigma_{\rho K^* \rightarrow \pi K} v_{\rho K^*} \rangle n_\rho n_{K^*} \\
& + \langle \sigma_{\pi \bar{K} \rightarrow \rho \bar{K}^*} v_{\pi \bar{K}} \rangle n_\pi n_{\bar{K}} - \langle \sigma_{\rho \bar{K}^* \rightarrow \pi \bar{K}} v_{\rho \bar{K}^*} \rangle n_\rho n_{\bar{K}^*} \\
& + \langle \sigma_{\pi K^* \rightarrow \rho K^*} v_{\pi K^*} \rangle n_\pi n_{K^*} - \langle \sigma_{\rho K^* \rightarrow \pi K^*} v_{\rho K^*} \rangle n_\rho n_{K^*} \\
& + \langle \sigma_{\pi \bar{K}^* \rightarrow \rho \bar{K}^*} v_{\pi \bar{K}^*} \rangle n_\pi n_{\bar{K}^*} - \langle \sigma_{\rho \bar{K}^* \rightarrow \pi \bar{K}^*} v_{\rho \bar{K}^*} \rangle n_\rho n_{\bar{K}^*} \\
& + \langle \sigma_{K \bar{K}^* \rightarrow \pi \rho} v_{K \bar{K}^*} \rangle n_K n_{\bar{K}^*} - \langle \sigma_{\pi \rho \rightarrow K \bar{K}^*} v_{\pi \rho} \rangle n_\pi n_\rho \\
& + \langle \sigma_{K^* \bar{K} \rightarrow \pi \rho} v_{K^* \bar{K}} \rangle n_{K^*} n_{\bar{K}} - \langle \sigma_{\pi \rho \rightarrow K^* \bar{K}} v_{\pi \rho} \rangle n_\pi n_\rho \\
& + 2 \langle \sigma_{K \bar{K} \rightarrow \rho\rho} v_{K \bar{K}} \rangle n_K n_{\bar{K}} - 2 \times \frac{1}{2} \langle \sigma_{\rho\rho \rightarrow K \bar{K}} v_{\rho\rho} \rangle n_\rho^2, \tag{3}
\end{aligned}$$

$$\begin{aligned}
\Psi_K = & 2 \times \frac{1}{2} \langle \sigma_{K^* K^* \rightarrow K K} v_{K^* K^*} \rangle n_{K^*}^2 - 2 \times \frac{1}{2} \langle \sigma_{K K \rightarrow K^* K^*} v_{K K} \rangle n_K^2 \\
& + \frac{1}{2} \langle \sigma_{K^* K^* \rightarrow K K^*} v_{K^* K^*} \rangle n_{K^*}^2 - \langle \sigma_{K K^* \rightarrow K^* K^*} v_{K K^*} \rangle n_K n_{K^*} \\
& + \langle \sigma_{K^* \bar{K}^* \rightarrow K \bar{K}} v_{K^* \bar{K}^*} \rangle n_{K^*} n_{\bar{K}^*} - \langle \sigma_{K \bar{K} \rightarrow K^* \bar{K}^*} v_{K \bar{K}} \rangle n_K n_{\bar{K}} \\
& + \langle \sigma_{K^* \bar{K}^* \rightarrow K \bar{K}^*} v_{K^* \bar{K}^*} \rangle n_{K^*} n_{\bar{K}^*} - \langle \sigma_{K \bar{K}^* \rightarrow K^* \bar{K}^*} v_{K \bar{K}^*} \rangle n_K n_{\bar{K}^*} \\
& + \langle \sigma_{\pi K^* \rightarrow \rho K} v_{\pi K^*} \rangle n_\pi n_{K^*} - \langle \sigma_{\rho K \rightarrow \pi K^*} v_{\rho K} \rangle n_\rho n_K \\
& + \langle \sigma_{\rho K^* \rightarrow \pi K} v_{\rho K^*} \rangle n_\rho n_{K^*} - \langle \sigma_{\pi K \rightarrow \rho K^*} v_{\pi K} \rangle n_\pi n_K \\
& + \langle \sigma_{\rho K^* \rightarrow \rho K} v_{\rho K^*} \rangle n_\rho n_{K^*} - \langle \sigma_{\rho K \rightarrow \rho K^*} v_{\rho K} \rangle n_\rho n_K \\
& + \frac{1}{2} \langle \sigma_{\pi\pi \rightarrow K \bar{K}} v_{\pi\pi} \rangle n_\pi^2 - \langle \sigma_{K \bar{K} \rightarrow \pi\pi} v_{K \bar{K}} \rangle n_K n_{\bar{K}} \\
& + \langle \sigma_{\pi\rho \rightarrow K \bar{K}^*} v_{\pi\rho} \rangle n_\pi n_\rho - \langle \sigma_{K \bar{K}^* \rightarrow \pi\rho} v_{K \bar{K}^*} \rangle n_K n_{\bar{K}^*} \\
& + \frac{1}{2} \langle \sigma_{\rho\rho \rightarrow K \bar{K}} v_{\rho\rho} \rangle n_\rho^2 - \langle \sigma_{K \bar{K} \rightarrow \rho\rho} v_{K \bar{K}} \rangle n_K n_{\bar{K}}, \tag{4}
\end{aligned}$$

$$\begin{aligned}
\Psi_{K^*} = & 2 \times \frac{1}{2} \langle \sigma_{KK \rightarrow K^* K^*} v_{KK} \rangle n_K^2 - 2 \times \frac{1}{2} \langle \sigma_{K^* K^* \rightarrow KK} v_{K^* K^*} \rangle n_{K^*}^2 \\
& + \langle \sigma_{KK^* \rightarrow K^* K^*} v_{KK^*} \rangle n_K n_{K^*} - \frac{1}{2} \langle \sigma_{K^* K^* \rightarrow KK^*} v_{K^* K^*} \rangle n_{K^*}^2 \\
& + \langle \sigma_{K\bar{K} \rightarrow K^* \bar{K}^*} v_{K\bar{K}} \rangle n_K n_{\bar{K}} - \langle \sigma_{K^* \bar{K}^* \rightarrow K\bar{K}} v_{K^* \bar{K}^*} \rangle n_{K^*} n_{\bar{K}^*} \\
& + \langle \sigma_{K\bar{K}^* \rightarrow K^* \bar{K}^*} v_{K\bar{K}^*} \rangle n_K n_{\bar{K}^*} - \langle \sigma_{K^* \bar{K}^* \rightarrow K\bar{K}^*} v_{K^* \bar{K}^*} \rangle n_{K^*} n_{\bar{K}^*} \\
& + \langle \sigma_{\rho K \rightarrow \pi K^*} v_{\rho K} \rangle n_\rho n_K - \langle \sigma_{\pi K^* \rightarrow \rho K} v_{\pi K^*} \rangle n_\pi n_{K^*} \\
& + \langle \sigma_{\pi K \rightarrow \rho K^*} v_{\pi K} \rangle n_\pi n_K - \langle \sigma_{\rho K^* \rightarrow \pi K} v_{\rho K^*} \rangle n_\rho n_{K^*} \\
& + \langle \sigma_{\rho K \rightarrow \rho K^*} v_{\rho K} \rangle n_\rho n_K - \langle \sigma_{\rho K^* \rightarrow \rho K} v_{\rho K^*} \rangle n_\rho n_{K^*} \\
& + \langle \sigma_{\pi \rho \rightarrow K^* \bar{K}} v_{\pi \rho} \rangle n_\pi n_\rho - \langle \sigma_{K^* \bar{K} \rightarrow \pi \rho} v_{K^* \bar{K}} \rangle n_{K^*} n_{\bar{K}}.
\end{aligned} \tag{5}$$

The source term of  $\bar{K}$  ( $\bar{K}^*$ ) is not shown since  $\Psi_{\bar{K}}$  ( $\Psi_{\bar{K}^*}$ ) is obtained from  $\Psi_K$  ( $\Psi_{K^*}$ ) by the replacements of the subscripts,  $K \leftrightarrow \bar{K}$  and  $K^* \leftrightarrow \bar{K}^*$ . Those terms what contain the factor 2 relate to the reactions that have two indistinguishable initial or final mesons. This factor means that the two initial mesons of a species vanish to attain no final mesons of the species or the two final mesons of a species appear from no initial mesons of the species. The first fourteen terms of  $\Psi_\pi$  equal the negative of the first fourteen terms of  $\Psi_\rho$ . The first fourteen terms of  $\Psi_K$  equal the negative of the first fourteen terms of  $\Psi_{K^*}$ . The quark-interchange processes are only contained in these terms. Therefore, the quark-interchange processes contribute to the variations of the number densities of  $\pi$  and  $\rho$ , or  $K$  and  $K^*$ , in equal magnitudes but opposite signs.

The thermal averaged cross section with the relative velocity of two initial mesons  $v_{\text{rel}}$  is defined as

$$\langle \sigma_{ij \rightarrow i'j'} v_{\text{rel}} \rangle = \frac{\int \frac{d^3 k_1}{(2\pi)^3} f_i(k_1) \frac{d^3 k_2}{(2\pi)^3} f_j(k_2) \sigma_{ij \rightarrow i'j'}(\sqrt{s}) v_{\text{rel}}}{\int \frac{d^3 k_1}{(2\pi)^3} f_i(k_1) \int \frac{d^3 k_2}{(2\pi)^3} f_j(k_2)}, \tag{6}$$

where  $f_i(k_1)$  and  $f_j(k_2)$  are the momentum distributions of the two initial mesons with the four-momenta  $k_1$  and  $k_2$ , respectively;  $\sigma_{ij \rightarrow i'j'}(\sqrt{s})$  is a cross section that depends on the center-of-mass energy  $\sqrt{s}$  of the two initial mesons. We take the approximate factorization form of the Jüttner distribution with nonequilibrium fugacity  $\lambda_i$  of particle species  $i$ ,

$$f_i(k) = \frac{\lambda_i}{e^{u \cdot k/T} - 1}, \tag{7}$$

where  $T$  is temperature. If two initial mesons are indistinguishable,  $f_i$  and  $f_j$  possess the same fugacity and as seen in Eqs. (2)-(5) a factor of  $\frac{1}{2}$  is in some terms to remove the double counting of initial mesons in the thermal average.

The number density of particle species  $i$  is given by

$$n_i = g_i \int \frac{d^3 k}{(2\pi)^3} \frac{\lambda_i}{e^{u \cdot k/T} - 1} = u^0 \lambda_i \bar{n}_i, \tag{8}$$

with

$$\bar{n}_i = \frac{g_i}{2\pi^2} \int_0^\infty d|\vec{k}'| \frac{\vec{k}'^2}{e^{\sqrt{\vec{k}'^2 + m_i^2}/T} - 1}, \quad (9)$$

where  $m_i$  is the mass of particle species  $i$ ; the spin-isospin degeneracy factor  $g_i = 3$  for  $\pi$ , 9 for  $\rho$ , 2 for  $K$  or  $\bar{K}$ , 6 for  $K^*$  or  $\bar{K}^*$ ;  $\vec{k}'$  is the particle momentum in the local comoving reference frame. The derivative of  $\bar{n}_i$  with respect to  $T$  is

$$\frac{d\bar{n}_i}{dT} = \frac{1}{T} (3\bar{n}_i + \bar{n}_{i-}), \quad (10)$$

with

$$\bar{n}_{i-} = \frac{g_i}{2\pi^2} \int_0^\infty d|\vec{k}'| \frac{m_i^2}{e^{\sqrt{\vec{k}'^2 + m_i^2}/T} - 1}. \quad (11)$$

For symmetric matter  $\lambda_{\bar{K}} = \lambda_K$ ,  $\lambda_{\bar{K}^*} = \lambda_{K^*}$ ,  $\bar{n}_{\bar{K}} = \bar{n}_K$ ,  $\bar{n}_{\bar{K}^*} = \bar{n}_{K^*}$ ,  $\bar{n}_{\bar{K}-} = \bar{n}_{K-}$  and  $\bar{n}_{\bar{K}^*-} = \bar{n}_{K^*-}$ .

Inserting Eqs. (8) and (10) into Eqs. (2)-(5), we obtain rate equations for fugacities of  $\pi$ ,  $\rho$ ,  $K$  and  $K^*$  of symmetric matter in the longitudinal expansion

$$\begin{aligned} & \frac{\dot{\lambda}_\pi}{\lambda_\pi} + \left(3 + \frac{\bar{n}_{\pi-}}{\bar{n}_\pi}\right) \frac{\dot{T}}{T} + \frac{1}{\tau} \\ &= 2 \times \frac{1}{2} \langle \sigma_{\rho\rho \rightarrow \pi\pi} v_{\rho\rho} \rangle u^0 \frac{\lambda_\rho^2 \bar{n}_\rho^2}{\lambda_\pi \bar{n}_\pi} - 2 \times \frac{1}{2} \langle \sigma_{\pi\pi \rightarrow \rho\rho} v_{\pi\pi} \rangle u^0 \lambda_\pi \bar{n}_\pi \\ &+ 2 \langle \sigma_{\rho K \rightarrow \pi K^*} v_{\rho K} \rangle u^0 \frac{\lambda_\rho \bar{n}_\rho \lambda_K \bar{n}_K}{\lambda_\pi \bar{n}_\pi} - 2 \langle \sigma_{\pi K^* \rightarrow \rho K} v_{\pi K^*} \rangle u^0 \lambda_{K^*} \bar{n}_{K^*} \\ &+ 2 \langle \sigma_{\rho K^* \rightarrow \pi K} v_{\rho K^*} \rangle u^0 \frac{\lambda_\rho \bar{n}_\rho \lambda_{K^*} \bar{n}_{K^*}}{\lambda_\pi \bar{n}_\pi} - 2 \langle \sigma_{\pi K \rightarrow \rho K^*} v_{\pi K} \rangle u^0 \lambda_K \bar{n}_K \\ &+ 2 \langle \sigma_{\rho K^* \rightarrow \pi K^*} v_{\rho K^*} \rangle u^0 \frac{\lambda_\rho \bar{n}_\rho \lambda_{K^*} \bar{n}_{K^*}}{\lambda_\pi \bar{n}_\pi} - 2 \langle \sigma_{\pi K^* \rightarrow \rho K^*} v_{\pi K^*} \rangle u^0 \lambda_{K^*} \bar{n}_{K^*} \\ &+ 2 \langle \sigma_{K\bar{K} \rightarrow \pi\pi} v_{K\bar{K}} \rangle u^0 \frac{\lambda_K^2 \bar{n}_K^2}{\lambda_\pi \bar{n}_\pi} - 2 \times \frac{1}{2} \langle \sigma_{\pi\pi \rightarrow K\bar{K}} v_{\pi\pi} \rangle u^0 \lambda_\pi \bar{n}_\pi \\ &+ 2 \langle \sigma_{K\bar{K}^* \rightarrow \pi\rho} v_{K\bar{K}^*} \rangle u^0 \frac{\lambda_K \bar{n}_K \lambda_{K^*} \bar{n}_{K^*}}{\lambda_\pi \bar{n}_\pi} - 2 \langle \sigma_{\pi\rho \rightarrow K\bar{K}^*} v_{\pi\rho} \rangle u^0 \lambda_\rho \bar{n}_\rho, \end{aligned} \quad (12)$$



$$\begin{aligned}
& \frac{\dot{\lambda}_\rho}{\lambda_\rho} + \left(3 + \frac{\bar{n}_{\rho-}}{\bar{n}_\rho}\right) \frac{\dot{T}}{T} + \frac{1}{\tau} \\
&= 2 \times \frac{1}{2} \langle \sigma_{\pi\pi \rightarrow \rho\rho} v_{\pi\pi} \rangle u^0 \frac{\lambda_\pi^2 \bar{n}_\pi^2}{\lambda_\rho \bar{n}_\rho} - 2 \times \frac{1}{2} \langle \sigma_{\rho\rho \rightarrow \pi\pi} v_{\rho\rho} \rangle u^0 \lambda_\rho \bar{n}_\rho \\
&\quad + 2 \langle \sigma_{\pi K^* \rightarrow \rho K} v_{\pi K^*} \rangle u^0 \frac{\lambda_\pi \bar{n}_\pi \lambda_{K^*} \bar{n}_{K^*}}{\lambda_\rho \bar{n}_\rho} - 2 \langle \sigma_{\rho K \rightarrow \pi K^*} v_{\rho K} \rangle u^0 \lambda_{K^*} \bar{n}_K \\
&\quad + 2 \langle \sigma_{\pi K \rightarrow \rho K^*} v_{\pi K} \rangle u^0 \frac{\lambda_\pi \bar{n}_\pi \lambda_K \bar{n}_K}{\lambda_\rho \bar{n}_\rho} - 2 \langle \sigma_{\rho K^* \rightarrow \pi K} v_{\rho K^*} \rangle u^0 \lambda_{K^*} \bar{n}_{K^*} \\
&\quad + 2 \langle \sigma_{\pi K^* \rightarrow \rho K^*} v_{\pi K^*} \rangle u^0 \frac{\lambda_\pi \bar{n}_\pi \lambda_{K^*} \bar{n}_{K^*}}{\lambda_\rho \bar{n}_\rho} - 2 \langle \sigma_{\rho K^* \rightarrow \pi K^*} v_{\rho K^*} \rangle u^0 \lambda_{K^*} \bar{n}_{K^*} \\
&\quad + 2 \langle \sigma_{K\bar{K}^* \rightarrow \pi\rho} v_{K\bar{K}^*} \rangle u^0 \frac{\lambda_K \bar{n}_K \lambda_{K^*} \bar{n}_{K^*}}{\lambda_\rho \bar{n}_\rho} - 2 \langle \sigma_{\pi\rho \rightarrow K\bar{K}^*} v_{\pi\rho} \rangle u^0 \lambda_\pi \bar{n}_\pi \\
&\quad + 2 \langle \sigma_{K\bar{K} \rightarrow \rho\rho} v_{K\bar{K}} \rangle u^0 \frac{\lambda_K^2 \bar{n}_K^2}{\lambda_\rho \bar{n}_\rho} - 2 \times \frac{1}{2} \langle \sigma_{\rho\rho \rightarrow K\bar{K}} v_{\rho\rho} \rangle u^0 \lambda_\rho \bar{n}_\rho, \tag{13}
\end{aligned}$$

$$\begin{aligned}
& \frac{\dot{\lambda}_K}{\lambda_K} + \left(3 + \frac{\bar{n}_{K-}}{\bar{n}_K}\right) \frac{\dot{T}}{T} + \frac{1}{\tau} \\
&= 2 \times \frac{1}{2} \langle \sigma_{K^* K^* \rightarrow K K} v_{K^* K^*} \rangle u^0 \frac{\lambda_{K^*}^2 \bar{n}_{K^*}^2}{\lambda_K \bar{n}_K} - 2 \times \frac{1}{2} \langle \sigma_{K K \rightarrow K^* K^*} v_{K K} \rangle u^0 \lambda_K \bar{n}_K \\
&\quad + \frac{1}{2} \langle \sigma_{K^* K^* \rightarrow K K} v_{K^* K^*} \rangle u^0 \frac{\lambda_{K^*}^2 \bar{n}_{K^*}^2}{\lambda_K \bar{n}_K} - \langle \sigma_{K K^* \rightarrow K^* K^*} v_{K K^*} \rangle u^0 \lambda_{K^*} \bar{n}_{K^*} \\
&\quad + \langle \sigma_{K^* \bar{K}^* \rightarrow K \bar{K}} v_{K^* \bar{K}^*} \rangle u^0 \frac{\lambda_{K^*}^2 \bar{n}_{K^*}^2}{\lambda_K \bar{n}_K} - \langle \sigma_{K \bar{K} \rightarrow K^* \bar{K}^*} v_{K \bar{K}} \rangle u^0 \lambda_K \bar{n}_K \\
&\quad + \langle \sigma_{K^* \bar{K}^* \rightarrow K \bar{K}} v_{K^* \bar{K}^*} \rangle u^0 \frac{\lambda_{K^*}^2 \bar{n}_{K^*}^2}{\lambda_K \bar{n}_K} - \langle \sigma_{K \bar{K}^* \rightarrow K^* \bar{K}^*} v_{K \bar{K}^*} \rangle u^0 \lambda_{K^*} \bar{n}_{K^*} \\
&\quad + \langle \sigma_{\pi K^* \rightarrow \rho K} v_{\pi K^*} \rangle u^0 \frac{\lambda_\pi \bar{n}_\pi \lambda_{K^*} \bar{n}_{K^*}}{\lambda_K \bar{n}_K} - \langle \sigma_{\rho K \rightarrow \pi K^*} v_{\rho K} \rangle u^0 \lambda_\rho \bar{n}_\rho \\
&\quad + \langle \sigma_{\rho K^* \rightarrow \pi K} v_{\rho K^*} \rangle u^0 \frac{\lambda_\rho \bar{n}_\rho \lambda_{K^*} \bar{n}_{K^*}}{\lambda_K \bar{n}_K} - \langle \sigma_{\pi K \rightarrow \rho K^*} v_{\pi K} \rangle u^0 \lambda_\pi \bar{n}_\pi \\
&\quad + \langle \sigma_{\rho K^* \rightarrow \rho K} v_{\rho K^*} \rangle u^0 \frac{\lambda_\rho \bar{n}_\rho \lambda_{K^*} \bar{n}_{K^*}}{\lambda_K \bar{n}_K} - \langle \sigma_{\rho K \rightarrow \rho K^*} v_{\rho K} \rangle u^0 \lambda_\rho \bar{n}_\rho \\
&\quad + \frac{1}{2} \langle \sigma_{\pi\pi \rightarrow K\bar{K}} v_{\pi\pi} \rangle u^0 \frac{\lambda_\pi^2 \bar{n}_\pi^2}{\lambda_K \bar{n}_K} - \langle \sigma_{K\bar{K} \rightarrow \pi\pi} v_{K\bar{K}} \rangle u^0 \lambda_K \bar{n}_K \\
&\quad + \langle \sigma_{\pi\rho \rightarrow K\bar{K}^*} v_{\pi\rho} \rangle u^0 \frac{\lambda_\pi \bar{n}_\pi \lambda_\rho \bar{n}_\rho}{\lambda_K \bar{n}_K} - \langle \sigma_{K\bar{K}^* \rightarrow \pi\rho} v_{K\bar{K}^*} \rangle u^0 \lambda_{K^*} \bar{n}_{K^*} \\
&\quad + \frac{1}{2} \langle \sigma_{\rho\rho \rightarrow K\bar{K}} v_{\rho\rho} \rangle u^0 \frac{\lambda_\rho^2 \bar{n}_\rho^2}{\lambda_K \bar{n}_K} - \langle \sigma_{K\bar{K} \rightarrow \rho\rho} v_{K\bar{K}} \rangle u^0 \lambda_K \bar{n}_K, \tag{14}
\end{aligned}$$

$$\begin{aligned}
& \frac{\dot{\lambda}_{K^*}}{\lambda_{K^*}} + \left(3 + \frac{\bar{n}_{K^*-}}{\bar{n}_{K^*}}\right) \frac{\dot{T}}{T} + \frac{1}{\tau} \\
&= 2 \times \frac{1}{2} \langle \sigma_{KK \rightarrow K^*K^*} v_{KK} \rangle u^0 \frac{\lambda_K^2 \bar{n}_K^2}{\lambda_{K^*} \bar{n}_{K^*}} - 2 \times \frac{1}{2} \langle \sigma_{K^*K^* \rightarrow KK} v_{K^*K^*} \rangle u^0 \lambda_{K^*} \bar{n}_{K^*} \\
&\quad + \langle \sigma_{KK^* \rightarrow K^*K^*} v_{KK^*} \rangle u^0 \lambda_K \bar{n}_K - \frac{1}{2} \langle \sigma_{K^*K^* \rightarrow KK^*} v_{K^*K^*} \rangle u^0 \lambda_{K^*} \bar{n}_{K^*} \\
&\quad + \langle \sigma_{K\bar{K} \rightarrow K^*\bar{K}^*} v_{K\bar{K}} \rangle u^0 \frac{\lambda_K^2 \bar{n}_K^2}{\lambda_{K^*} \bar{n}_{K^*}} - \langle \sigma_{K^*\bar{K}^* \rightarrow K\bar{K}} v_{K^*\bar{K}^*} \rangle u^0 \lambda_{K^*} \bar{n}_{K^*} \\
&\quad + \langle \sigma_{K\bar{K}^* \rightarrow K^*\bar{K}} v_{K\bar{K}^*} \rangle u^0 \lambda_K \bar{n}_K - \langle \sigma_{K^*\bar{K} \rightarrow K\bar{K}^*} v_{K^*\bar{K}} \rangle u^0 \lambda_{K^*} \bar{n}_{K^*} \\
&\quad + \langle \sigma_{\rho K \rightarrow \pi K^*} v_{\rho K} \rangle u^0 \frac{\lambda_\rho \bar{n}_\rho \lambda_K \bar{n}_K}{\lambda_{K^*} \bar{n}_{K^*}} - \langle \sigma_{\pi K^* \rightarrow \rho K} v_{\pi K^*} \rangle u^0 \lambda_\pi \bar{n}_\pi \\
&\quad + \langle \sigma_{\pi K \rightarrow \rho K^*} v_{\pi K} \rangle u^0 \frac{\lambda_\pi \bar{n}_\pi \lambda_K \bar{n}_K}{\lambda_{K^*} \bar{n}_{K^*}} - \langle \sigma_{\rho K^* \rightarrow \pi K} v_{\rho K^*} \rangle u^0 \lambda_\rho \bar{n}_\rho \\
&\quad + \langle \sigma_{\rho K \rightarrow \rho K^*} v_{\rho K} \rangle u^0 \frac{\lambda_\rho \bar{n}_\rho \lambda_K \bar{n}_K}{\lambda_{K^*} \bar{n}_{K^*}} - \langle \sigma_{\rho K^* \rightarrow \rho K} v_{\rho K^*} \rangle u^0 \lambda_\rho \bar{n}_\rho \\
&\quad + \langle \sigma_{\pi \rho \rightarrow K^*\bar{K}} v_{\pi \rho} \rangle u^0 \frac{\lambda_\pi \bar{n}_\pi \lambda_\rho \bar{n}_\rho}{\lambda_{K^*} \bar{n}_{K^*}} - \langle \sigma_{K^*\bar{K} \rightarrow \pi \rho} v_{K^*\bar{K}} \rangle u^0 \lambda_K \bar{n}_K, \tag{15}
\end{aligned}$$

where the overdots denote the derivative with respect to the proper time  $\tau$ .

For the purpose of studying the role of quark-interchange processes, it is enough to only consider the longitudinal expansion of hadronic matter. The relativistic hydrodynamic equation is

$$\partial_\mu T^{\mu\nu} = 0, \tag{16}$$

where  $T^{\mu\nu}$  is the energy-momentum tensor given by

$$T^{\mu\nu} = (\epsilon + P)u^\mu u^\nu - P g^{\mu\nu}, \tag{17}$$

where  $\epsilon$  is energy density and  $P$  is pressure. The simple form of  $T^{\mu\nu}$  above holds for an ideal fluid where viscosity effects have been neglected. The Bjorken's scaling solution of the hydrodynamic equation is [29]

$$\frac{d\epsilon}{d\tau} + \frac{\epsilon + P}{\tau} = 0. \tag{18}$$

The energy density is

$$\epsilon = \epsilon_\pi + \epsilon_\rho + \epsilon_K + \epsilon_{\bar{K}} + \epsilon_{K^*} + \epsilon_{\bar{K}^*} \tag{19}$$

where  $\epsilon_\pi$ ,  $\epsilon_\rho$ ,  $\epsilon_K$ ,  $\epsilon_{\bar{K}}$ ,  $\epsilon_{K^*}$  and  $\epsilon_{\bar{K}^*}$  are the energy densities of  $\pi$ ,  $\rho$ ,  $K$ ,  $\bar{K}$ ,  $K^*$  and  $\bar{K}^*$ , respectively. In order to solve Eq. (18), relation of pressure and energy density is needed. Detailed studies [30–33] have shown that the relation can be  $P = 0.15\epsilon$ . Once cross sections for the reactions concerned are known, Eqs. (12)–(15) and (18) determine time dependence of  $T(\tau)$ ,  $\lambda_\pi(\tau)$ ,  $\lambda_\rho(\tau)$ ,  $\lambda_K(\tau)$  and  $\lambda_{K^*}(\tau)$ .

### 3 Cross sections for meson-meson reactions

The meson-meson cross sections entailed in the master rate equations in Section 2 are the isospin-averaged cross sections that are obtained by taking the average over the isospin states of the two initial mesons and the sum over the isospin states of the two final mesons

$$\sigma_{ij \rightarrow i'j'}(\sqrt{s}) = \frac{1}{(2I_1 + 1)(2I_2 + 1)} \sum_I (2I + 1) \sigma(I, \sqrt{s}), \quad (20)$$

where  $I_1$  and  $I_2$  are the isospins of the two initial mesons, respectively, and  $\sigma(I, \sqrt{s})$  is the spin-averaged cross section for the reaction with the total isospin  $I$ .

We explicitly decompose the cross section  $\sigma(I, \sqrt{s})$  into three parts: the first is  $\sigma_{\text{qi}}$  from the quark-interchange process, the second  $\sigma_{\text{anni}}$  from the annihilation processes and the third  $\sigma_{\text{res}}$  from the resonant processes. Since the momenta and the coordinates of the quark and antiquark constituents of the final mesons in the quark-interchange process  $A(q_1 \bar{q}_1) + B(q_2 \bar{q}_2) \rightarrow C(q_1 \bar{q}_2) + D(q_2 \bar{q}_1)$  are different from those in the annihilation processes or the resonant processes  $A(q_1 \bar{q}_1) + B(q_2 \bar{q}_2) \rightarrow C(q_1 \bar{q}_1) + D(q_2 \bar{q}_2)$ , there is no interference between the quark-interchange process and the annihilation processes and between the quark-interchange process and the resonant processes. No interference of the annihilation processes and the resonant processes is usually assumed. Then the cross section for a reaction is written as

$$\sigma(I, \sqrt{s}) = c_{\text{qi}} \sigma_{\text{qi}}(I, \sqrt{s}) + c_{\text{anni}} \sigma_{\text{anni}}(I, \sqrt{s}) + c_{\text{res}} \sigma_{\text{res}}(I, \sqrt{s}). \quad (21)$$

The coefficients  $c_{\text{qi}}$ ,  $c_{\text{anni}}$  and  $c_{\text{res}}$  that take values of 0 or 1 are listed in Table 1. In the following three subsections  $\sigma_{\text{qi}}$ ,  $\sigma_{\text{anni}}$  and  $\sigma_{\text{res}}$  are presented. For two isospin channels all the three processes contribute. For most isospin channels only the quark-interchange processes or the annihilation processes contribute. Quark-interchange-induced reactions refer to the channels where only the quark interchange works. The quark-interchange processes include the quark-interchange-induced reactions.

#### 3.1 Cross sections for quark-interchange processes

In Ref. [26] we have obtained unpolarized cross sections for some meson-meson nonresonant reactions governed only by the quark-interchange mechanism. The cross sections rely on mesonic quark-antiquark wave functions and constituent-constituent interaction. The quark-antiquark relative-motion wave functions are determined by the Buchmüller-Tye potential [34] that arises from color confinement and one-gluon exchange plus one- and

two-loop corrections. The constituent-constituent interaction includes the Buchmüller-Tye potential what is nonrelativistic, central and spin-independent, and spin-spin terms that are obtained by performing Foldy-Wouthuysen canonical transformations to a relativistic two-constituent Hamiltonian that includes the linear confinement and a relativistic one-gluon-exchange potential plus perturbative one- and two-loop corrections [35]. The wave functions and the interaction can reproduce the experimental mass splittings between the ground-state pseudoscalar octet mesons and the ground-state vector nonet mesons [35]. The wave functions and the interaction were employed [26] to calculate cross sections for nonresonant reactions  $A(q_1\bar{q}_1) + B(q_2\bar{q}_2) \rightarrow C(q_1\bar{q}_2) + D(q_2\bar{q}_1)$  which are endothermic or exothermic. The  $\sqrt{s}$ -dependence of numerical cross sections exhibited in Ref. [26] show a peak for each of endothermic reactions and large magnitudes very near the threshold energies of exothermic reactions. For convenient use of the numerical cross sections in solving the master rate equations, parametrizations similar to Ref. [36] read

$$\sigma_{\text{qi}}(I, \sqrt{s}) = \sigma_{\text{max}} \left( \frac{\epsilon}{\epsilon_{\text{endo}}} \right)^a \exp \left[ a \left( 1 - \frac{\epsilon}{\epsilon_{\text{endo}}} \right) \right], \quad (22)$$

where  $\epsilon = \sqrt{s} - \sqrt{s_0}$  shows difference from the threshold energy  $\sqrt{s_0}$ . Values for the parameters  $\sigma_{\text{max}}$ ,  $\epsilon_{\text{endo}}$  and  $a$  for the quark-interchange-induced endothermic reactions given in the introduction are shown in Table 2.

The right-hand side of Eq. (22) indicates the zero value of cross section at the threshold energy and a fall of cross section at  $\sqrt{s} \rightarrow \infty$ .  $\epsilon_{\text{endo}}$  is close to the center-of-mass energy at which an endothermic reaction reaches maximum cross section  $\sigma_{\text{max}}$ . The power function and the exponential function do leave a curve that is not symmetric with respect to the peak. The peak is in the energy region that is accessible to meson-meson reactions in mesonic matter.

Table 2 shows the channels with the highest isospins. Since quark-interchange processes can also take place in low isospin channels as seen in Table 1, flavor matrix elements  $f_{\text{flavor}}(I)$  of the quark-interchange processes are listed in Table 3 for different isospins. The entry  $f_{\text{flavor}}(1) = 0$  for  $\pi\pi \rightarrow \rho\rho$  for  $I = 1$  means that the reaction in  $I = 1$  is forbidden. This is consistent with the fact that the antisymmetric state of  $\pi\pi$  is not allowed. The discrepancy of the cross sections for different isospin channels of a reaction results from the different flavor matrix elements while matrix elements involving spin and spatial wave functions are equal. Then, for instance, we have  $\sigma_{\text{qi}}(I = 0, \sqrt{s}) = \frac{1}{4}\sigma_{\text{qi}}(I = 2, \sqrt{s})$  and  $\sigma_{\text{qi}}(I = 1, \sqrt{s}) = 0$  for  $\pi\pi \rightarrow \rho\rho$ . Let  $I_{\text{max}}$  denote the highest isospin of a reaction. The cross section for a channel listed in Table 3 is

$$\sigma_{\text{qi}}(I, \sqrt{s}) = \frac{f_{\text{flavor}}^2(I)}{f_{\text{flavor}}^2(I_{\text{max}})} \sigma_{\text{qi}}(I_{\text{max}}, \sqrt{s}). \quad (23)$$

The cross section for an exothermic reaction  $i'(S_3I_3) + j'(S_4I_4) \rightarrow i(S_1I_1) + j(S_2I_2)$  is obtained from the endothermic reaction  $ij \rightarrow i'j'$  by the detailed balance

$$\sigma_{i'j' \rightarrow ij} = \frac{\vec{P}^2}{\vec{P}'^2} \frac{g_i}{g_f} \sigma_{ij \rightarrow i'j'}, \quad (24)$$

where  $g_i = (2S_1+1)(2I_1+1)(2S_2+1)(2I_2+1)$  and  $g_f = (2S_3+1)(2I_3+1)(2S_4+1)(2I_4+1)$  denote the spin-isospin degeneracy factors of initial particles with the spins  $S_1$  and  $S_2$  as well as the isospins  $I_1$  and  $I_2$ , and of final particles with the spins  $S_3$  and  $S_4$  as well as the isospins  $I_3$  and  $I_4$ , respectively;  $\vec{P}$  and  $\vec{P}'$  denote momenta of an initial meson and a final meson in the center-of-momentum frame of the reaction  $ij \rightarrow i'j'$ , respectively.

### 3.2 Cross sections for annihilation processes

The isospin-averaged cross section for an annihilation reaction can be parametrized by [37, 38]

$$\sigma_{\text{anni}}(\sqrt{s}) = b \left(1 - \frac{s_0}{s}\right)^c. \quad (25)$$

Values of the parameter  $b$  and the dimensionless parameter  $c$  for the reactions  $\pi\pi \rightarrow K\bar{K}$ ,  $\pi\rho \rightarrow K\bar{K}^*(K^*\bar{K})$  and  $K\bar{K} \rightarrow \rho\rho$  are given in Table 4. Since no experimental data are available, we assume that cross sections for other annihilation processes listed in Table 1 possess Eq. (25) with the same parameters  $b$  and  $c$  as the reaction  $\pi\pi \rightarrow K\bar{K}$ . The treatment of the annihilation processes is simple.

### 3.3 Cross sections for resonant processes

Cross sections for resonant processes are generally described by the Breit-Wigner formula [1, 2, 5–7]

$$\sigma_{\text{res}}(\sqrt{s}) = \frac{2J+1}{(2S_1+1)(2S_2+1)} \frac{\pi}{\vec{P}^2} \frac{\Gamma^2 B_{\text{in}} B_{\text{out}}}{(\sqrt{s} - m_{\text{R}})^2 + \Gamma^2/4}, \quad (26)$$

where a resonance has its spin  $J$ , its energy  $m_{\text{R}}$  and its full width  $\Gamma$ , and  $B_{\text{in}}$  and  $B_{\text{out}}$  are the branching fractions of the resonance decays into the initial state and the final state, respectively. We take account of the resonances  $f_0(1370)$ ,  $\rho(1450)$ ,  $f_0(1500)$  and  $\rho_3(1690)$  for  $\pi\pi \leftrightarrow \rho\rho$ ,  $K_1(1270)$ ,  $K_1(1400)$ ,  $K^*(1410)$ ,  $K_2^*(1430)$ ,  $K^*(1680)$  and  $K_3^*(1780)$  for  $\pi K^* \leftrightarrow \rho K$ ,  $f_0(980)$ ,  $\phi(1020)$ ,  $f_2(1270)$ ,  $f_0(1370)$ ,  $\rho(1450)$ ,  $f_0(1500)$ ,  $f_2'(1525)$ ,  $\rho_3(1690)$ ,  $\rho(1700)$ ,  $f_0(1710)$ ,  $f_2(1810)$  and  $f_4(2050)$  for  $\pi\pi \leftrightarrow K\bar{K}$ . Since the full widths and the branching fractions for some resonances have not been fixed by measurements [39], their values we select for the reactions  $\pi\pi \leftrightarrow \rho\rho$ ,  $\pi K^* \leftrightarrow \rho K$  and  $\pi\pi \leftrightarrow K\bar{K}$  are listed in Table 5.

## 4 Results and discussions

In this section we represent and discuss results that are from solving the master rate equations in combination with the hydrodynamic equation (18) simultaneously by numerical integration using a fourth order Runge-Kutta method. The inelastic 2-to-2 scattering in the master rate equations includes the three types of processes: the quark-interchange processes, the annihilation processes and the resonant processes. As a good approximation, we assume that hadronization of quark-gluon plasma at the critical temperature  $T_c = 175$  MeV [40] only produces  $\pi$ ,  $\rho$ ,  $K$ ,  $\bar{K}$ ,  $K^*$  and  $\bar{K}^*$ . We assume that the hadronization is finished at  $\tau_h = 5.6$  fm/ $c$  and at the moment mesonic matter has  $\lambda_\pi = 0.7$ ,  $\lambda_\rho = 0.7$ ,  $\lambda_K = 0.5$  and  $\lambda_{K^*} = 0.2$  for the fugacities of  $\pi$ ,  $\rho$ ,  $K$  and  $K^*$ , respectively. We consider mesonic matter at or near mid-rapidity, i.e.,  $u^\mu \approx (1, 0, 0, 0)$ , solve Eqs. (12)-(15) and (18), and terminate numerical calculations when mesonic matter reaches the kinetic freeze-out temperature  $T_{fz} = 105$  MeV, which corresponds to a freeze-out time of the order of 30 fm/ $c$ .

If the inelastic 2-to-2 scattering is switched off, ie., the source terms are zero, the master rate equations become

$$\partial_\mu(n_i u^\mu) = 0, \quad (27)$$

which have the solutions

$$n_i \sim \frac{1}{\tau}. \quad (28)$$

Together with Eq. (8) we have

$$\lambda_i \sim \frac{1}{u^0 \bar{n}_i \tau}. \quad (29)$$

For massive bosons,  $\bar{n}_i$  given by Eq. (9) and energy densities do not simply rely on a power of  $T$ , and the hydrodynamic equation cannot guarantee  $\bar{n}_i \tau$  as constants. Therefore,  $\lambda_i$  depend on the proper time  $\tau$  unlike the case of massless bosons which fugacities are constants. Fugacities for  $\pi$ ,  $\rho$ ,  $K$  and  $K^*$  are denoted by  $\lambda_{\pi\text{no}}$ ,  $\lambda_{\rho\text{no}}$ ,  $\lambda_{K\text{no}}$  and  $\lambda_{K^*\text{no}}$ , respectively, and are plotted as solid curves in Fig. 1. The solid curves for  $\rho$ ,  $K$  and  $K^*$  rise with the increase of time. The fugacity of the lightest meson first decreases slightly and then increases. Compared to the results in the absence of the source terms, we show meson fugacities by the dashed curves and indicate the meson fugacities by  $\lambda_{i\text{qar}}$  ( $i = \pi, \rho, K, K^*$ ) while the quark-interchange processes, the annihilation processes and the resonant processes are all included. The differences between  $\lambda_{i\text{qar}}$  and  $\lambda_{i\text{no}}$  due to the inelastic 2-to-2 scattering are obvious. To show how the quark-interchange processes modify fugacities, we show the fugacities by dotted curves and denote the fugacities by  $\lambda_{i\text{qi}}$  ( $i = \pi, \rho, K, K^*$ ) while only the quark-interchange processes govern time dependence

of the fugacities. In most of the range  $5.6 \text{ fm}/c < \tau < 30 \text{ fm}/c$  the absolute values of the fugacity differences,  $|\lambda_{iqi} - \lambda_{ino}|$ , caused by the quark-interchange processes are smaller than  $|\lambda_{iqar} - \lambda_{ino}|$  caused by the three types of processes.

To show a role of the quark-interchange processes, we define

$$R_i = \frac{\lambda_{iqi} - \lambda_{ino}}{\lambda_{iqar} - \lambda_{ino}}. \quad (30)$$

The larger the absolute values of  $R_i$ , the more important the quark-interchange processes. If  $R_i > 0$ , either of the quark-interchange processes and the combination of the three types of processes increases (reduces) fugacities relative to  $\lambda_{ino}$ . If  $R_i < 0$ , the quark-interchange processes increase (reduce) fugacities relative to  $\lambda_{ino}$  while the annihilation and resonant processes reduce (increase) fugacities. Values of  $R_i$  change with the increase of time. At  $\tau = 20 \text{ fm}/c$ ,  $R_\pi = 0.37$ ,  $R_\rho = 0.30$ ,  $R_K = 0.21$  and  $R_{K^*} = 0.27$ .

To quantitatively determine the importance of the quark-interchange processes, we define the average of the absolute value of  $R_i$  by

$$\bar{R}_i = \frac{\int_{\tau_h}^{\tau_{fz}} d\tau |R_i|}{\tau_{fz} - \tau_h}. \quad (31)$$

where  $\tau_{fz}$  is the freeze-out time of mesonic matter. Then,  $\bar{R}_\pi = 0.53$ ,  $\bar{R}_\rho = 0.30$ ,  $\bar{R}_K = 0.21$  and  $\bar{R}_{K^*} = 0.27$ . Hence, with the set of initial fugacities,  $\lambda_\pi = 0.7$ ,  $\lambda_\rho = 0.7$ ,  $\lambda_K = 0.5$  and  $\lambda_{K^*} = 0.2$ , for the master rate equations and the hydrodynamic equation, the quark-interchange processes are important in the contribution of the inelastic 2-to-2 scattering to the evolution of mesonic matter. But the conclusion is only limited to this set. We need to examine  $\bar{R}_i$  versus other initial fugacities. Initial fugacities of mesonic matter depend on incident energies in nucleus-nucleus collisions. The Au-Au collisions have been carried out at various energies of per pair of colliding nucleons allowed by the Relativistic Heavy Ion Collider (RHIC) and Pb-Pb collisions at the Large Hadron Collider (LHC) have been performed at higher energies. Different nucleus-nucleus collisions at different energies produce mesonic matter with different magnitudes of initial fugacities. Therefore, we use a wide range of initial fugacities to check the importance of the quark-interchange processes. It is impossible to plot graphs for  $\bar{R}_i$  ( $i = \pi, \rho, K, K^*$ ) versus the four variables  $\lambda_\pi, \lambda_\rho, \lambda_K$  and  $\lambda_{K^*}$ , but we can tabulate  $\bar{R}_i$  ( $i = \pi, \rho, K, K^*$ ) versus a finite sets of initial fugacities in the range between 0 and 1. We take 81 sets in which  $\lambda_\pi = 0.35, 0.65, 0.95$ ,  $\lambda_\rho = 0.15, 0.45, 0.75$ ,  $\lambda_K = 0.25, 0.55, 0.85$  and  $\lambda_{K^*} = 0.15, 0.55, 0.95$ . Statistically, the 81 sets can tell us how important the quark-interchange processes are. The freeze-out time  $\tau_{fz}$  depends on initial fugacities. Averages  $\bar{R}_i$  ( $i = \pi, \rho, K, K^*$ ) for the 81 sets of initial fugacities are listed in the middle four columns in Tables 6-8.

The average may be as large as 33.07 and this occurs when the contributions of the quark-interchange, annihilation and resonant processes can cancel each other. The average may be as small as 0.01. Most of the entries in the middle four columns are above 0.2. Therefore, the quark-interchange processes are important in the contribution of the inelastic 2-to-2 scattering to the evolution of mesonic matter.

Via HIJING Monte Carlo simulations [41–43], initial fugacities of deconfined gluons and quarks produced in central Au-Au collisions at  $\sqrt{s_{NN}} = 200$  GeV are about 0.2 and 0.032, respectively, as seen in the second set of initial conditions of quark-gluon plasma in Table I of Ref. [44]. Using the ratio 0.2 of strange-quark number to up-quark number [45], that may reproduce the measured ratios  $K^-/\pi^- = 0.15 \pm 0.02$  and  $K^{*0}/K^- = 0.205 \pm 0.033$  at midrapidity [46], we solve master rate equations of quark-gluon plasma given in Ref. [47] to obtain time dependence of fugacities of gluons and quarks. We obtain the time  $\tau_h \approx 5.6$  fm/c, the fugacities  $\lambda_g \approx 0.75$  and  $\lambda_q \approx 0.52$  at  $T_c$ . Coalescence of quarks and antiquarks forms mesons at  $T_c$ . Assume that the formed mesons are only  $\pi$ ,  $\rho$ ,  $K$ ,  $\bar{K}$ ,  $K^*$  and  $\bar{K}^*$  and that  $\lambda_\pi = \lambda_\rho$  and  $\lambda_K = \lambda_{K^*}$  at  $T_c$ . Then we obtain  $\lambda_\pi = \lambda_\rho \approx 1.31$  and  $\lambda_K = \lambda_{K^*} \approx 0.56$  that are the initial fugacities of mesonic matter produced in central Au-Au collisions at  $\sqrt{s_{NN}} = 200$  GeV. For other nucleus-nucleus collisions meson fugacities are different from these values. The pion fugacity may not equal the rho fugacity at  $T_c$  and the kaon fugacity may not equal the vector kaon fugacity. If  $\sqrt{s_{NN}}$  decreases continuously, meson fugacities decrease continuously. Therefore,  $\lambda_\pi = \lambda_\rho = 0.7$ ,  $\lambda_K = 0.5$  and  $\lambda_{K^*} = 0.2$  used in this section and some sets of initial fugacities listed in Tables 6-8 can be covered in some nucleus-nucleus collisions at some values of  $\sqrt{s_{NN}}$ . Since the strange-quark number is less than half the up-quark number, those sets of initial fugacities in which both  $\lambda_K$  and  $\lambda_{K^*}$  are larger than  $\lambda_\pi$  and  $\lambda_\rho$  are not possible. But such sets of initial fugacities yield  $\bar{R}_i > 0.2$  ( $i = \pi, \rho, K, K^*$ ) in more than half the entries of  $\bar{R}_i$ . Therefore, the impossible sets of initial fugacities help us more firmly establish that the quark-interchange processes are important in the contribution of the inelastic 2-to-2 scattering to the evolution of mesonic matter.

It is shown in Table 1 that fourteen reaction channels involve the quark-interchange processes, sixteen channels the annihilation processes and three channels the resonant processes. In a reaction where a quark-interchange process occurs, the channel with the highest isospin is only induced by the quark-interchange process and the number  $2I + 1$  of isospin component in Eq. (20) can enhance the capability of the process in influencing the evolution of mesonic matter.



## 5 Results pertinent to $2 \leftrightarrow 1$ processes

Since we only consider  $\pi$ ,  $\rho$ ,  $K$ ,  $\bar{K}$ ,  $K^*$  and  $\bar{K}^*$ , resonances involved are  $\rho$ ,  $K^*$  and  $\bar{K}^*$ . Then we include  $\pi\pi \leftrightarrow \rho$ ,  $\pi K \leftrightarrow K^*$  and  $\pi\bar{K} \leftrightarrow \bar{K}^*$ . Let  $\Gamma_{\rho \rightarrow \pi\pi}$ ,  $\Gamma_{K^* \rightarrow \pi K}$  and  $\Gamma_{\bar{K}^* \rightarrow \pi\bar{K}}$  be the decay widths of  $\rho \rightarrow \pi\pi$ ,  $K^* \rightarrow \pi K$  and  $\bar{K}^* \rightarrow \pi\bar{K}$ , respectively. We add the following four expressions

$$\begin{aligned} & 2\Gamma_{\rho \rightarrow \pi\pi}n_\rho - 2 \times \frac{1}{2} \langle \sigma_{\pi\pi \rightarrow \rho} v_{\pi\pi} \rangle n_\pi n_\pi + \Gamma_{K^* \rightarrow \pi K} n_{K^*} + \Gamma_{\bar{K}^* \rightarrow \pi\bar{K}} n_{\bar{K}^*} \\ & - \langle \sigma_{\pi K \rightarrow K^*} v_{\pi K} \rangle n_\pi n_K - \langle \sigma_{\pi\bar{K} \rightarrow \bar{K}^*} v_{\pi\bar{K}} \rangle n_\pi n_{\bar{K}}, \\ & - \Gamma_{\rho \rightarrow \pi\pi} n_\rho + \frac{1}{2} \langle \sigma_{\pi\pi \rightarrow \rho} v_{\pi\pi} \rangle n_\pi n_\pi, \\ & \Gamma_{K^* \rightarrow \pi K} n_{K^*} - \langle \sigma_{\pi K \rightarrow K^*} v_{\pi K} \rangle n_\pi n_K, \end{aligned}$$

and

$$- \Gamma_{K^* \rightarrow \pi K} n_{K^*} + \langle \sigma_{\pi K \rightarrow K^*} v_{\pi K} \rangle n_\pi n_K,$$

to the source terms  $\Psi_\pi$ ,  $\Psi_\rho$ ,  $\Psi_K$  and  $\Psi_{K^*}$  in Eqs. (2)-(5), respectively, to establish master rate equations with the  $2 \leftrightarrow 1$  mesonic processes. Obtained from the experimental data [48], the cross section for  $\pi\pi \rightarrow \rho$  is

$$\sigma_{\pi\pi \rightarrow \rho} = \frac{80 \text{ mb}}{1 + 4(\sqrt{s} - m_\rho)^2 / \Gamma_{\rho \rightarrow \pi\pi}^2}. \quad (32)$$

The cross section for  $\pi K \rightarrow K^*$  or  $\pi\bar{K} \rightarrow \bar{K}^*$  can be found in Refs. [3,4]. From solutions of the master rate equations with the  $2 \leftrightarrow 1$  processes and the hydrodynamic equation (18), we get the average values  $\bar{R}_i$  at various initial fugacities and list them in the right four columns in Tables 6-8.

In the tables about 96% of the entries in the right four columns have values larger than 0.5 and 53% larger than 1. Moreover, most of  $\bar{R}_i$  ( $i = \pi, \rho, K, K^*$ ) are larger than the corresponding ones derived from the master rate equations without the  $2 \leftrightarrow 1$  processes. Therefore, while the quark-antiquark annihilation processes and the resonant processes are taken into account, the quark-interchange processes must be included on an equal footing.

## 6 Results pertinent to transverse expansion

In the preceding sections we have considered only the longitudinal expansion for mesonic matter. In this section we rely on both longitudinal and transverse expansion to deal with mesonic matter produced in central collisions. The four-velocity of the local

reference frame is  $u^\mu = \gamma(\frac{t}{\tau}, v_r, 0, \frac{z}{\tau})$  with  $\gamma = 1/\sqrt{1-v_r^2}$ , where  $v_r$  is the transverse velocity. The left-hand side in Eq. (1) becomes

$$\partial_\mu(n_i u^\mu) = \gamma \frac{\partial n_i}{\partial \tau} + n_i \left( \frac{\partial \gamma}{\partial \tau} + \frac{\gamma}{\tau} \right) + \frac{1}{r} \frac{\partial}{\partial r} (r n_i \gamma v_r). \quad (33)$$

For matter uniformly distributed,

$$\partial_\mu(n_i u^\mu) = \gamma \frac{\partial n_i}{\partial \tau} + n_i \gamma^3 v_r \frac{\partial v_r}{\partial \tau} + n_i \gamma (2\gamma^2 v_r^2 + 1) \frac{\partial v_r}{\partial r} + \frac{n_i \gamma}{\tau} + \frac{n_i \gamma v_r}{r}. \quad (34)$$

In terms of fugacities,

$$\partial_\mu(n_i u^\mu) = u^0 \bar{n}_i \gamma \frac{\partial \lambda_i}{\partial \tau} + u^0 \lambda_i \gamma \frac{\partial \bar{n}_i}{\partial T} \frac{\partial T}{\partial \tau} + 2n_i \gamma^3 v_r \frac{\partial v_r}{\partial \tau} + n_i \gamma (2\gamma^2 v_r^2 + 1) \frac{\partial v_r}{\partial r} + \frac{n_i \gamma}{\tau} + \frac{n_i \gamma v_r}{r}. \quad (35)$$

Solving the master rate equations with Eq. (35) and the  $2 \leftrightarrow 1$  mesonic processes and the hydrodynamic equations describing the longitudinal and transverse expansion in Ref. [49], we obtain, for example, at  $\lambda_\pi = 0.7$ ,  $\lambda_\rho = 0.7$ ,  $\lambda_K = 0.5$  and  $\lambda_{K^*} = 0.2$ , the average values  $\bar{R}_i$  ( $i = \pi, \rho, K, K^*$ ) are 1.11, 0.78, 1.21 and 0.85, respectively. Corresponding to most sets of the initial fugacities listed in Tables 6-8,  $\bar{R}_\pi$ ,  $\bar{R}_\rho$ ,  $\bar{R}_K$  and  $\bar{R}_{K^*}$  are larger than 1. Therefore, we must use the quark-interchange processes on an equal footing while the annihilation processes and the resonant processes are considered.

## 7 Summary

We have established a set of master rate equations that describe time dependence of fugacities of pions, rhos, kaons and vector kaons in mesonic matter. A meson-meson reaction is comprised of the quark-interchange process, the annihilation processes and the resonant processes. The cross sections for the quark-interchange-induced reactions, that were obtained from the Buchmüller-Tye potential plus the spin-spin interaction, are parametrized for convenient use in studying the evolution of mesonic matter.

The variations of fugacities of pions, rhos, kaons and vector kaons are governed by the inelastic meson-meson scattering, the  $2 \leftrightarrow 1$  mesonic processes and the expansion of mesonic matter. In most reactions the quark-interchange processes take place. If the number density of  $\pi$  is increased (reduced) by the quark-interchange processes, the number density of  $\rho$  is reduced (increased) in the same amount. This relation also holds true for  $K$  and  $K^*$ . Numerical results of the master rate equations show that the quark-interchange processes are important in the contribution of the inelastic 2-to-2 scattering to the evolution of mesonic matter.

## Acknowledgments

This work was supported by National Natural Science Foundation of China under Grant No. 10675079.

# References

- [1] H. Sorge, H. Stöcker, W. Greiner, Ann. Phys. **192**, 266 (1989).
- [2] H. Sorge, Phys. Rev. C **52**, 3291 (1995).
- [3] B.-A. Li, C.M. Ko, Phys. Rev. C **52**, 2037 (1995).
- [4] Z.-W. Lin, C.M. Ko, B.-A. Li, B. Zhang, S. Pal, Phys. Rev. C **72**, 064901 (2005).
- [5] W. Cassing, E.L. Bratkovskaya, Phys. Rep. **308**, 65 (1999).
- [6] S.A. Bass *et al.*, Prog. Part. Nucl. Phys. **41**, 255 (1998).
- [7] C. Nonaka, S.A. Bass, Phys. Rev. C **75**, 014902 (2007).
- [8] D.E. Kahana, S.H. Kahana, Phys. Rev. C **58**, 3574 (1998).
- [9] D.E. Kahana, S.H. Kahana, Phys. Rev. C **59**, 1651 (1999).
- [10] B.-H. Sa, A. Tai, Comput. Phys. Commun. **90**, 121 (1995).
- [11] A. Tai, B.-H. Sa, Comput. Phys. Commun. **116**, 353 (1999).
- [12] T.J. Humanic, Phys. Rev. C **57**, 866 (1998).
- [13] Y. Nara, N. Otuka, A. Ohnishi, K. Niita, S. Chiba, Phys. Rev. C **61**, 024901 (1999).
- [14] T. Hirano, U. Heinz, D. Kharzeev, R. Lacey, Y. Nara, Phys. Lett. B **636**, 299 (2006).
- [15] L. Alvarez-Ruso, V. Koch, Phys. Rev. C **65**, 054901 (2002).
- [16] S. Gavin, Nucl. Phys. B **351**, 561 (1991).
- [17] C. Song, V. Koch, Phys. Rev. C **55**, 3026 (1997).
- [18] S. Pratt, K. Haglin, Phys. Rev. C **59**, 3304 (1999).
- [19] S.S. Adler *et al.* (PHENIX Collaboration), Phys. Rev. C **69**, 034909 (2004).
- [20] C. Adler *et al.* (STAR Collaboration), Phys. Lett. B **595**, 143 (2004).
- [21] I. Arsene *et al.* (BRAHMS Collaboration), Nucl. Phys. A **757**, 1 (2005).
- [22] B. B. Back *et al.* (PHOBOS Collaboration), Nucl. Phys. A **757**, 28 (2005).
- [23] J. Adams *et al.* (STAR Collaboration), Phys. Rev. Lett. **92**, 092301 (2004).
- [24] C. Amsler, N.A. Törnqvist, Phys. Rep. **389**, 61 (2004).
- [25] D.V. Bugg, Phys. Rep. **397**, 257 (2004).
- [26] Y.-Q. Li, X.-M. Xu, Nucl. Phys. A **794**, 210 (2007).
- [27] T. Barnes, E.S. Swanson, Phys. Rev. D **46**, 131 (1992).
- [28] E.S. Swanson, Ann. Phys. **220**, 73 (1992).
- [29] J.D. Bjorken, Phys. Rev. D **27**, 140 (1983).
- [30] H. Sorge, Phys. Lett. B **402**, 251 (1997).

- [31] L.V. Bravina *et al.*, Phys. Rev. C **60**, 024904 (1999).
- [32] P.F. Kolb, J. Sollfrank, U. Heinz, Phys. Lett. B **459**, 667 (1999).
- [33] P.F. Kolb, J. Sollfrank, U. Heinz, Phys. Rev. C **62**, 054909 (2000).
- [34] W. Buchmüller, S.-H.H. Tye, Phys. Rev. D **24**, 132 (1981).
- [35] X.-M. Xu, Nucl. Phys. A **697**, 825 (2002).
- [36] T. Barnes, E.S. Swanson, C.-Y. Wong, X.-M. Xu, Phys. Rev. C **68**, 014903 (2003).
- [37] G.E. Brown, C.M. Ko, Z.G. Wu, L.H. Xia, Phys. Rev. C **43**, 1881 (1991).
- [38] W. Cassing, E.L. Bratkovskaya, U. Mosel, S. Teis, A. Sibirtsev, Nucl. Phys. A **614**, 415 (1997).
- [39] Particle Data Group, W.-M. Yao *et al.*, J. Phys. G **33**, 1 (2006).
- [40] F. Karsch, E. Laermann, A. Peikert, Nucl. Phys. B **605**, 579 (2001).
- [41] X.-N. Wang, M. Gyulassy, Phys. Rev. D **44**, 3501 (1991).
- [42] M. Gyulassy, X.-N. Wang, Comput. Phys. Commun. **83**, 307 (1994).
- [43] X.-N. Wang, Phys. Rep. **280**, 287 (1997).
- [44] X.-M. Xu, D. Kharzeev, H. Satz, X.-N. Wang, Phys. Rev. C **53**, 3051 (1996).
- [45] T.S. Biró, P. Lévai, J. Zimányi, Phys. Rev. C **59**, 1574 (1999).
- [46] O. Barannikova, for the STAR Collaboration, arXiv:nucl-ex/0403014v1.
- [47] P. Lévai, B. Müller, X.-N. Wang, Phys. Rev. C **51**, 3326 (1995).
- [48] V. Flaminio, W.G. Moorhead, D.R.O. Morrison, N. Rivoire, CERN, Geneva Report No. CERN-HERA-84-01, 1984.
- [49] H. von Gersdorff, L. McLerran, M. Kataja, P.V. Ruuskanen, Phys. Rev. D **34**, 794 (1986).

Table 1: Values of  $c_{\text{qi}}$ ,  $c_{\text{anni}}$  and  $c_{\text{res}}$ .

Channel	$c_{\text{qi}}$	$c_{\text{anni}}$	$c_{\text{res}}$
$I = 2 \pi\pi \leftrightarrow \rho\rho$	1	0	0
$I = 1 \pi\pi \leftrightarrow \rho\rho$	0	1	0
$I = 0 \pi\pi \leftrightarrow \rho\rho$	1	1	1
$I = 1 KK \leftrightarrow K^*K^*$	1	0	0
$I = 0 KK \leftrightarrow K^*K^*$	1	0	0
$I = 1 KK^* \leftrightarrow K^*K^*$	1	0	0
$I = 0 KK^* \leftrightarrow K^*K^*$	1	0	0
$I = 1 K\bar{K} \leftrightarrow K^*\bar{K}^*$	0	1	0
$I = 0 K\bar{K} \leftrightarrow K^*\bar{K}^*$	0	1	0
$I = 1 K\bar{K}^* \leftrightarrow K^*\bar{K}^*$	0	1	0
$I = 0 K\bar{K}^* \leftrightarrow K^*\bar{K}^*$	0	1	0
$I = 3/2 \pi K^* \leftrightarrow \rho K$	1	0	0
$I = 1/2 \pi K^* \leftrightarrow \rho K$	1	1	1
$I = 3/2 \pi K \leftrightarrow \rho K^*$	1	0	0
$I = 1/2 \pi K \leftrightarrow \rho K^*$	1	1	0
$I = 3/2 \pi K^* \leftrightarrow \rho K^*$	1	0	0
$I = 1/2 \pi K^* \leftrightarrow \rho K^*$	1	1	0
$I = 3/2 \rho K \leftrightarrow \rho K^*$	1	0	0
$I = 1/2 \rho K \leftrightarrow \rho K^*$	1	1	0
$I = 1 \pi\pi \leftrightarrow K\bar{K}$	0	1	0
$I = 0 \pi\pi \leftrightarrow K\bar{K}$	0	1	1
$I = 1 \pi\rho \leftrightarrow K\bar{K}^*$	0	1	0
$I = 0 \pi\rho \leftrightarrow K\bar{K}^*$	0	1	0
$I = 1 K\bar{K} \leftrightarrow \rho\rho$	0	1	0
$I = 0 K\bar{K} \leftrightarrow \rho\rho$	0	1	0

Table 2: Parameters in Eq. (22).

Channel	$\sigma_{\max}$ (mb)	$\epsilon_{\text{endo}}$ (GeV)	$a$
$I = 2 \pi\pi \rightarrow \rho\rho$	0.49991	0.20909	0.87446
$I = 1 KK \rightarrow K^*K^*$	0.61622	0.16539	0.4883
$I = 1 KK^* \rightarrow K^*K^*$	0.85168	0.26399	1.05175
$I = 3/2 \pi K^* \rightarrow \rho K$	1.40233	0.15023	1.07478
$I = 3/2 \pi K \rightarrow \rho K^*$	0.49839	0.12056	0.40939
$I = 3/2 \pi K^* \rightarrow \rho K^*$	0.49	0.21	0.88
$I = 3/2 \rho K \rightarrow \rho K^*$	0.5081	0.3166	1.89693

Table 3: Flavor matrix elements  $f_{\text{flavor}}(I)$ .

	$I = 0$	$I = 1$	$I = 2$	$I = 1/2$	$I = 3/2$
$\pi\pi \rightarrow \rho\rho$	$-1/2$	0	1		
$KK \rightarrow K^*K^*$	1	1			
$KK^* \rightarrow K^*K^*$	1	1			
$\pi K^* \rightarrow \rho K$				$-1/2$	1
$\pi K \rightarrow \rho K^*$				$-1/2$	1
$\pi K^* \rightarrow \rho K^*$				$-1/2$	1
$\rho K \rightarrow \rho K^*$				$-1/2$	1

Table 4: Values of  $b$  and  $c$ .

Reaction	$b$ (mb)	$c$
$\pi\pi \rightarrow K\bar{K}$	2.7	0.76
$\pi\rho \rightarrow K\bar{K}^*(K^*\bar{K})$	0.4	0.5
$K\bar{K} \rightarrow \rho\rho$	3.5	0.38

Table 5: Some resonances formed in  $\pi\pi \leftrightarrow \rho\rho$ ,  $\pi K^* \leftrightarrow \rho K$  and  $\pi\pi \leftrightarrow K\bar{K}$ .

Name	$\Gamma$ (MeV)	$B_{\pi\pi}$	$B_{\rho\rho}$
$f_0(1370)$	370	0.26	0.208
$\rho(1450)$	147	0.0672	0.02
Name	$\Gamma$ (MeV)	$B_{\pi K^*}$	$B_{\rho K}$
$K_1(1400)$	174	0.94	0.3
$K^*(1410)$	232	0.4	0.07
$K^*(1680)$	322	0.299	0.314
Name	$\Gamma$ (MeV)	$B_{\pi\pi}$	$B_{K\bar{K}}$
$f_0(980)$	70	0.755	0.245
$f_0(1370)$	370	0.203	0.35
$\rho(1450)$	147	0.0672	0.0016
$\rho(1700)$	250	0.2345	0.0412
$f_2(1810)$	197	0.0048	0.003



Table 6:  $\bar{R}_\pi$ ,  $\bar{R}_\rho$ ,  $\bar{R}_K$  and  $\bar{R}_{K^*}$  irrelevant and relevant to the  $2 \leftrightarrow 1$  processes are listed in the middle and right four columns, respectively. Initial fugacities are in the left four columns.

$\lambda_\pi$	$\lambda_\rho$	$\lambda_K$	$\lambda_{K^*}$	$\bar{R}_\pi$	$\bar{R}_\rho$	$\bar{R}_K$	$\bar{R}_{K^*}$	$\bar{R}_\pi$	$\bar{R}_\rho$	$\bar{R}_K$	$\bar{R}_{K^*}$
0.35	0.15	0.25	0.15	0.43	0.18	1.14	1.80	1.34	1.54	0.95	1.02
0.35	0.15	0.25	0.55	1.63	0.19	0.30	0.20	0.99	2.03	4.79	0.93
0.35	0.15	0.25	0.95	0.36	0.19	0.27	0.34	0.87	2.81	1.17	0.90
0.35	0.15	0.55	0.15	1.19	0.22	0.01	2.52	1.75	6.89	0.53	1.06
0.35	0.15	0.55	0.55	0.45	0.23	0.17	0.03	1.34	2.68	0.36	0.85
0.35	0.15	0.55	0.95	0.27	0.21	2.86	0.04	0.93	2.04	6.22	0.83
0.35	0.15	0.85	0.15	5.28	0.50	0.01	2.56	4.49	2.42	0.50	1.72
0.35	0.15	0.85	0.55	0.54	0.74	0.04	0.08	2.23	2.71	0.35	0.77
0.35	0.15	0.85	0.95	0.29	0.22	0.09	0.03	2.34	4.07	0.27	0.77
0.35	0.45	0.25	0.15	0.61	0.28	0.22	0.18	1.07	1.00	0.98	1.16
0.35	0.45	0.25	0.55	0.44	2.76	0.27	0.39	1.00	5.32	1.66	0.96
0.35	0.45	0.25	0.95	0.40	2.16	0.22	0.42	0.93	1.41	1.52	0.94
0.35	0.45	0.55	0.15	0.28	0.21	0.13	2.07	1.27	0.97	0.77	1.77
0.35	0.45	0.55	0.55	0.74	0.26	0.10	0.13	1.48	1.04	0.67	0.93
0.35	0.45	0.55	0.95	0.50	0.66	0.08	0.22	0.99	1.29	0.45	0.90
0.35	0.45	0.85	0.15	0.45	0.20	0.10	5.44	1.98	0.97	0.68	0.80
0.35	0.45	0.85	0.55	0.26	0.21	0.08	0.10	1.98	1.01	0.60	0.87
0.35	0.45	0.85	0.95	0.99	0.29	0.07	0.11	1.75	1.13	0.50	0.85
0.35	0.75	0.25	0.15	7.50	0.28	0.25	0.40	1.04	0.99	1.00	1.25
0.35	0.75	0.25	0.55	0.42	0.41	0.34	0.42	1.00	1.02	1.38	0.97
0.35	0.75	0.25	0.95	0.42	0.57	0.58	0.43	0.95	1.07	1.31	0.95
0.35	0.75	0.55	0.15	0.20	0.24	0.18	0.47	1.16	0.96	0.83	1.72
0.35	0.75	0.55	0.55	0.92	0.28	0.19	0.22	1.12	0.98	0.78	0.96
0.35	0.75	0.55	0.95	1.32	0.34	0.19	0.30	1.03	1.01	0.70	0.93
0.35	0.75	0.85	0.15	0.32	0.22	0.15	0.69	1.45	0.94	0.74	1.11
0.35	0.75	0.85	0.55	0.39	0.25	0.15	0.56	1.42	0.96	0.70	1.11
0.35	0.75	0.85	0.95	4.53	0.28	0.16	0.19	1.72	0.98	0.64	0.89

Table 7: The same as Table 6.

$\lambda_\pi$	$\lambda_\rho$	$\lambda_K$	$\lambda_{K^*}$	$\bar{R}_\pi$	$\bar{R}_\rho$	$\bar{R}_K$	$\bar{R}_{K^*}$	$\bar{R}_\pi$	$\bar{R}_\rho$	$\bar{R}_K$	$\bar{R}_{K^*}$
0.65	0.15	0.25	0.15	0.15	0.17	0.14	1.74	0.68	1.44	0.70	1.08
0.65	0.15	0.25	0.55	0.17	0.20	0.20	1.61	1.25	0.73	0.89	0.87
0.65	0.15	0.25	0.95	0.11	0.20	0.22	1.36	0.98	0.74	0.94	0.83
0.65	0.15	0.55	0.15	10.48	0.16	0.14	5.73	0.92	2.30	7.31	1.11
0.65	0.15	0.55	0.55	0.51	0.21	6.34	0.07	0.86	0.68	5.43	1.00
0.65	0.15	0.55	0.95	2.90	0.21	0.51	0.08	0.87	0.72	5.80	0.76
0.65	0.15	0.85	0.15	1.50	0.18	0.03	4.62	1.34	1.42	0.34	1.74
0.65	0.15	0.85	0.55	2.15	0.21	0.24	0.11	0.78	1.09	0.41	1.35
0.65	0.15	0.85	0.95	1.71	0.22	3.52	0.09	0.83	0.69	12.40	0.69
0.65	0.45	0.25	0.15	0.14	2.44	2.00	0.09	1.73	1.67	3.07	1.43
0.65	0.45	0.25	0.55	0.59	0.13	0.18	0.69	1.37	1.64	0.74	0.96
0.65	0.45	0.25	0.95	1.03	0.15	0.21	0.62	0.98	1.99	0.86	0.93
0.65	0.45	0.55	0.15	0.36	0.28	0.13	0.33	1.62	1.04	0.72	0.92
0.65	0.45	0.55	0.55	2.09	1.14	0.80	0.13	1.52	1.60	1.08	0.90
0.65	0.45	0.55	0.95	0.44	0.17	3.52	0.22	0.97	2.56	2.85	0.87
0.65	0.45	0.85	0.15	7.58	0.23	0.09	0.51	1.62	0.97	0.60	1.19
0.65	0.45	0.85	0.55	0.37	4.12	0.03	0.47	4.25	1.53	0.48	1.10
0.65	0.45	0.85	0.95	0.29	0.30	0.08	0.07	1.68	1.91	0.35	0.80
0.65	0.75	0.25	0.15	1.85	0.52	2.24	0.12	1.18	1.05	3.80	42.57
0.65	0.75	0.25	0.55	0.76	3.09	0.10	0.60	1.06	1.46	1.99	0.98
0.65	0.75	0.25	0.95	0.54	4.69	0.19	0.53	0.98	1.85	0.89	0.95
0.65	0.75	0.55	0.15	0.27	0.27	0.20	0.30	1.27	0.97	0.84	1.13
0.65	0.75	0.55	0.55	0.93	0.57	0.16	0.46	1.15	1.09	0.78	1.01
0.65	0.75	0.55	0.95	0.44	1.58	0.51	0.33	0.98	1.90	0.60	0.92
0.65	0.75	0.85	0.15	0.37	0.24	0.15	0.42	1.65	0.94	0.71	0.85
0.65	0.75	0.85	0.55	0.26	0.26	0.13	0.82	1.51	0.99	0.65	1.71
0.65	0.75	0.85	0.95	0.88	0.45	0.10	0.17	1.19	1.16	0.54	0.87

Table 8: The same as Table 6.

$\lambda_\pi$	$\lambda_\rho$	$\lambda_K$	$\lambda_{K^*}$	$\bar{R}_\pi$	$\bar{R}_\rho$	$\bar{R}_K$	$\bar{R}_{K^*}$	$\bar{R}_\pi$	$\bar{R}_\rho$	$\bar{R}_K$	$\bar{R}_{K^*}$
0.95	0.15	0.25	0.15	0.12	0.17	0.09	3.27	0.86	0.88	0.65	1.15
0.95	0.15	0.25	0.55	0.16	0.20	0.17	2.74	0.85	0.84	0.78	1.44
0.95	0.15	0.25	0.95	0.17	0.20	0.20	1.32	1.26	0.83	0.85	1.30
0.95	0.15	0.55	0.15	0.23	0.16	3.95	0.34	0.92	0.90	4.40	0.96
0.95	0.15	0.55	0.55	0.26	0.21	0.34	0.08	0.95	0.86	1.38	1.64
0.95	0.15	0.55	0.95	0.28	0.21	0.31	0.21	1.75	0.84	1.29	1.88
0.95	0.15	0.85	0.15	4.44	0.14	0.11	0.95	0.95	0.90	1.54	1.03
0.95	0.15	0.85	0.55	0.67	0.21	3.62	0.10	1.02	0.86	8.08	1.67
0.95	0.15	0.85	0.95	0.73	0.22	8.17	0.11	1.98	0.84	8.36	2.43
0.95	0.45	0.25	0.15	0.06	0.08	0.03	0.03	2.55	1.32	0.30	1.26
0.95	0.45	0.25	0.55	0.06	0.17	0.16	33.07	1.73	1.41	0.65	0.94
0.95	0.45	0.25	0.95	0.04	0.18	0.19	1.84	1.31	2.17	0.77	0.86
0.95	0.45	0.55	0.15	0.14	1.42	0.45	0.24	1.74	1.25	1.15	0.89
0.95	0.45	0.55	0.55	0.15	0.19	0.54	0.34	1.13	1.21	2.25	1.03
0.95	0.45	0.55	0.95	0.10	0.21	0.33	0.28	1.05	1.13	3.67	0.81
0.95	0.45	0.85	0.15	0.97	0.75	0.08	0.37	1.15	1.23	0.47	0.96
0.95	0.45	0.85	0.55	0.99	0.31	0.19	1.44	1.02	1.47	0.57	1.22
0.95	0.45	0.85	0.95	2.48	0.24	2.60	0.05	0.82	1.21	15.76	1.01
0.95	0.75	0.25	0.15	0.17	5.86	0.20	0.08	2.13	2.59	4.36	1.46
0.95	0.75	0.25	0.55	0.46	0.08	0.14	1.11	1.76	2.07	0.41	0.99
0.95	0.75	0.25	0.95	15.83	0.12	0.19	0.72	1.49	2.32	0.68	0.93
0.95	0.75	0.55	0.15	0.96	0.41	0.29	0.25	1.90	1.09	0.93	1.12
0.95	0.75	0.55	0.55	4.09	4.11	0.28	1.85	1.51	1.40	0.85	1.16
0.95	0.75	0.55	0.95	8.19	0.14	1.61	0.41	1.13	1.58	1.39	0.88
0.95	0.75	0.85	0.15	0.32	0.28	0.16	0.34	1.57	0.88	0.66	0.88
0.95	0.75	0.85	0.55	0.25	0.78	0.09	1.51	1.31	1.16	0.54	0.92
0.95	0.75	0.85	0.95	0.70	0.47	0.84	0.18	1.14	2.50	1.15	0.78

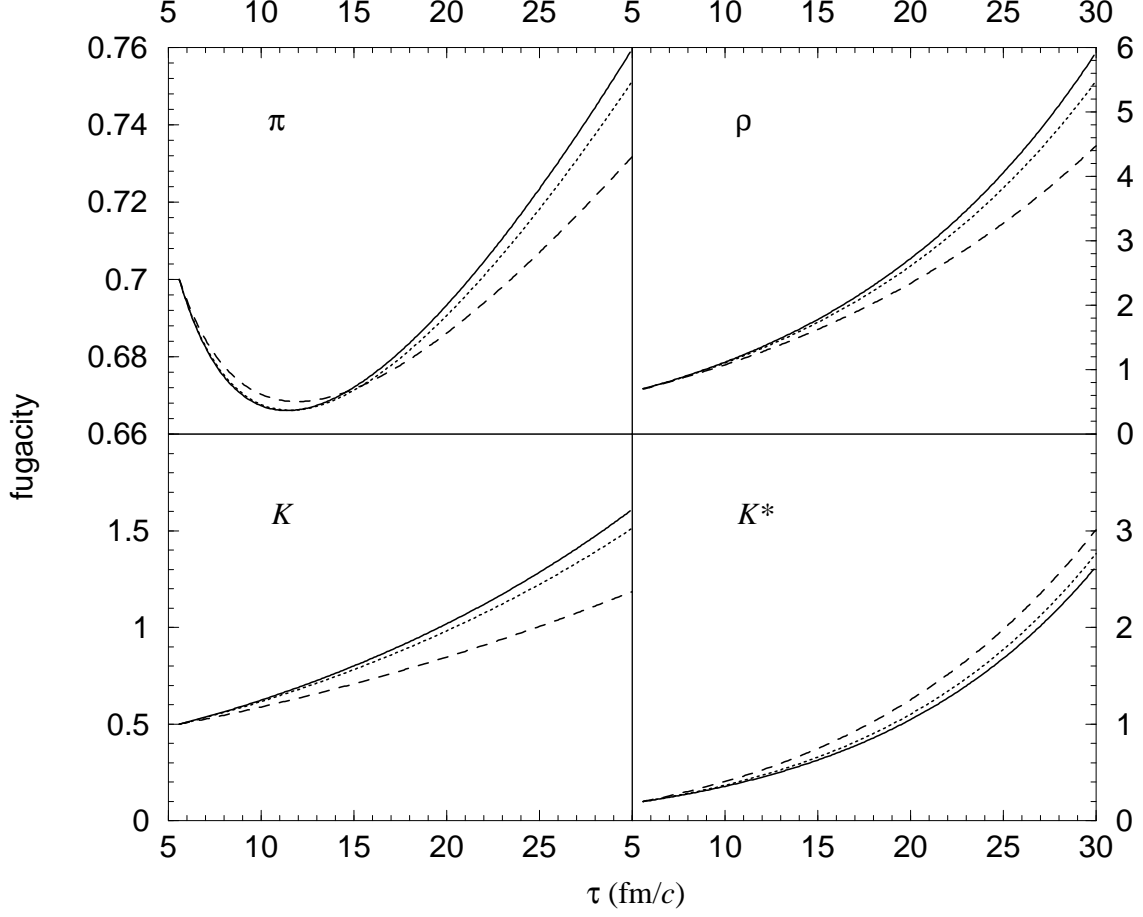


Figure 1: Time dependence of  $\lambda_\pi$ ,  $\lambda_\rho$ ,  $\lambda_K$  and  $\lambda_{K^*}$  without the source terms (solid curves), with the quark-interchange, annihilation and resonant processes (dashed curves) and with only the quark-interchange processes (dotted curves).